A consensus approach to PI gains tuning for quality-fair video delivery

Laura Dal Col, Sophie Tarbouriech, Luca Zaccarian, Michel Kieffer

INTERNATIONAL JOURNAL OF ROBUST AND NONLINEAR CONTROL
Int. J. Robust. Nonlinear Control 0000; **00**:1–19
Published online in Wiley InterScience (www.interscience.wiley.com). DOI: 10.1002/rnc

A Consensus Approach to PI Gains Tuning for Quality-Fair Video Delivery

Laura Dal Col[1] , Sophie Tarbouriech[2*] Luca Zaccarian [3], Michel Kieffer[4]

[1,2,3] *CNRS, LAAS and Univ. de Toulouse, Toulouse, France.*

[3] *Dipartimento di Ing. Industriale, University of Trento, Italy.*

[4] *L2S - CNRS - Univ Paris-Sud and Institut Universitaire de France, Gif-sur-Yvette, France.*

SUMMARY

In this paper we provide necessary and sufficient conditions for the quality-fair delivery of multimedia contents to mobile users. We control the encoding rates and the transmission rates of the video streams, delivered through a limited capacity channel. This problem is cast into a problem of consensus among identical discrete-time linear systems, connected through a network with fixed and fully connected topology. The information exchanged over the communication network is the measure of the quality of the encoded videos. Based on a consensus result for identical linear systems, we reduce the problem of designing the Proportional and Integral (PI) gains of the encoding rate and transmission rate controllers to a linear static output feedback. We propose an iterative design technique based on linear matrix inequalities to solve the corresponding nonconvex problem, thereby providing a constructive optimality-based approach to the PI gains tuning problem. We demonstrate the effectiveness of our method in simulations, where we compare it to pre-existing approaches. Copyright © 0000 John Wiley & Sons, Ltd.

Received ...

KEY WORDS: Consensus, controller design, fairness, video delivery

1. INTRODUCTION

In recent years video-on-demand has emerged as one of the most important applications of multimedia. The delivery of compressed videos has increased rapidly with the development of the wireless networks and the widespread use of smartphones [1]. Among all multimedia applications, videos require the largest amount of bandwidth. Being a scarce resource, efficient bandwidth utilization is the main concern in video broadcasting schemes. Moreover, operators have to satisfy application-layer quality-of-experience constraints, which are more challenging than traditional network-layer quality-of-service constraints.

In this paper we consider the problem of the parallel delivery of multiple encoded video streams to mobile users, through a dedicated broadcast channel of limited capacity. We want

*Correspondence to: Sophie Tarbouriech, LAAS-CNRS, 7 avenue du colonel Roche, F-31400 Toulouse, France and Université de Toulouse, CNRS, F-31400 Toulouse, France.
E-mail: [1] ldalcol@laas.fr, [2] tarbour@laas.fr, [3] zaccarian@laas.fr, [4] kieffer@lss.supelec.fr.

Contract/grant sponsor: Work supported by the grant OptHySYS founded by the Univeristy of Trento.

Contract/grant sponsor: Work supported by the ANR project LimICoS; contract/grant number: 12 BS03 005 01.

to provide the users with video contents of similar qualities. An allocation not accounting for the source characteristics may lead to unacceptable quality for high-complexity video compared to lower-complexity ones. Therefore, several alternative solutions have been proposed in the literature. In particular, [2] considers a utility max-min fair resource allocation, which tries to maximize the worst utility. Nevertheless, it does not consider the temporal variability of the rate-utility characteristics (RUC) of the contents, or the delays introduced by the network and the buffers of the delivery system. The work [3] presents a content-aware distortion-fair video delivery scheme, assuming that the characteristics of the video frames are known in advance. This restricts its usage to the streaming of stored videos. Lagrangian optimization frameworks are considered in [4, 5]. In [4], the sum of the achievable rates is maximized, while minimizing the distortion difference among streams. In [5], the average quality is maximized under total rate constraints, and constraints on the Peak Signal-to-Noise Ratio (PSNR) discrepancy between streams. Both approaches require to gather all RUCs of the streams at the control unit. The user experience is accurately modeled in [6] using the empirical cumulative distribution function of the predicted video quality. In [7, 8] a heuristic control approach based on Proportional Integral (PI) controllers is used to regulate the encoding rate of video servers and the transmission rate of the video streams towards the channel. In fact, if the videos are encoded at a constant bit-rate, the quality may change significantly with the variations of the characteristics of the contents. On the other hand, if the contents are encoded at a variable bit-rate, the buffering delay may increase significantly, leading to unacceptable delivery fluctuations. The joint actions of the controllers provide the desirable effect in terms of video-fairness: videos with utility below the average are drained faster through the corresponding buffers, and the encoding rate of such streams is then increased to improve the quality. In the scheme [7, 8] the control is performed in some Media Aware Network Element (MANE) [9] at the bottleneck of the links between the remote servers and the communication channel. The MANE is located close to the Base Station (BS), to which the clients are connected. In this *fully centralized* version of the controller, the MANE is in charge of sending the encoding rate target to each video server, based on the measure of the buffer level. On the contrary, in a *partially distributed* control architecture, the servers receive only the individual buffer discrepancies, and they are in charge of computing the encoding rate.

The main contribution of this paper is to provide a systematic and optimized method to perform the gain tuning of the PI quality-fair video streaming control proposed in [7, 8]. This result is obtained by casting the fair-delivery requirement into a problem of consensus among identical linear systems (or agents). *Consensus* refers to agents coming to a global agreement on a state value, by the exchange of information modeled by some communication graph. The range of examples of consensus and synchronization in modern control engineering is wide. Recently, consensus have been used to control for network clock synchronization in [10] and [11], for steering control of self-directed underwater gliders in [12], and to control the data flow and the failures in multi-hop control networks in [13], just to name a few. It has been shown in [14] that mild assumptions on the graph connectivity ensure uniform exponential consensus, see also [15, 16]. Consensus algorithms are primarily studied when the agents' open-loop dynamics are described by integrator chains (e.g. single- or double-integrator models [16, 17]). Recently the consensus problem has been investigated considering agents modeled by general linear time-invariant (LTI) systems [18, 19]. Consensus and synchronization problems are extensively studied in the literature for identical multi-agent systems, see, e.g., [20–22]. In [23], a state-feedback consensus protocol is proposed for linear multi-agent systems with switching topology. In [24], a linear quadratic regulator based optimal control approach was used for the controller design via state-feedback information. When the full state is not available, an observer can be used to estimate the states [25–27]. This makes the control architecture more complex. To overcome this problem, output-feedback based control may provide satisfactory solutions and some methods have been given in [28–30].

DOI: 10.1002/rnc

By applying the general consensus result of [31] for identical linear systems, we give here necessary and sufficient conditions for the synchronization among the quality measures of the delivered video streams. Our result has its roots in the existing works [19, 21, 32, 33]. We use a Lyapunov formulation, essentially providing a converse Lyapunov theorem for this application. Using these necessary and sufficient conditions, we can provide a systematic and optimized PI tuning procedure, based on a static output feedback design algorithm. The output feedback controller design problem is NP-hard [34]. In this paper we relax the output feedback design bilinear matrix inequalities using an iterative Linear Matrix Inequality (LMI) technique. Besides giving a comparable solutions to heuristic methods [7, 8, 35], our design technique exhibits desirable properties of initialization, stopping, and feasibility guarantees. Furthermore, applications of our algorithm are not limited to the quality-fair delivery problem, which makes it a relevant contribution of broader interest. In this paper we extend the preliminary results reported in [35] in several directions. We provide a self-contained proof of [35, Theorem 2], which was not present in the preliminary conference paper, and we extend the result by giving the explicit expression of a quadratic Lyapunov function for the system under consideration, thereby providing a converse Lyapunov theorem for consensus. We apply a new coordinate transformation to the system dynamics, which leads to a systematic tuning of the PI controller gains (rather than the ad-hoc one of our preliminary work [35]). In [35] we compared different PI tuning methods, here we extend the comparison to other controller types. In particular we compare the performance of PI controllers, tuned with our new method, with the PI controllers tuned as in [7], and with the controller schemes in [2] and [5].

The paper is organized as follows. Section 2 presents the the quality-fair video delivery problem. In Section 3 we cast the quality-fair video delivery problem into a consensus problem and we give necessary and sufficient conditions for consensus. In Section 4 a systematic method to design the controller gains is proposed using Finsler's lemma and LMI techniques. The effectiveness of this method is illustrated with simulations in Section 5. Concluding remarks end the paper.

Notation. We denote with $x^+(j) = x(j+1)$ the one-step forward shift operation for discrete-time systems. $\mathbf{1}_N$ indicates the N dimensional (column) vector with entries all equal to 1. Given a square matrix $A \in \Re^{n\times n}$, $\lambda(A)$ denotes the set of eigenvalues of A. The symbol $\mathbb{C}_{\leq\beta}$ denotes the set of the complex numbers with modulus less or equal to β.

Graph Theory. Let $\mathcal{G} = (\mathcal{V}, \mathcal{E}, A)$ be an undirected weighted graph. Any undirected graph $\mathcal{G}$ is described by a node set $\mathcal{V} = \{v_1, \ldots, v_N\}$, an edge set $\mathcal{E} = \{e_1, \ldots, e_N\} \subseteq \mathcal{V} \times \mathcal{V}$, whose elements specify the incidence relation between distinct pairs of nodes, and the adjacency matrix $A = [a_{ij}]$ with weighting factors $a_{ij} \geq 0$. The adjacency elements associated with the edges of the graph are positive, *i.e.*, $a_{ij} > 0$ if and only if $(v_i, v_j) \in \mathcal{E}$, otherwise $a_{ij} = 0$. The diagonal matrix $D = \text{diag}\{d_1, \ldots, d_N\}$ is the degree matrix of $\mathcal{G}$, whose diagonal elements are $d_i = \sum_{j=1}^{N} a_{ij}$. The corresponding Laplacian of $\mathcal{G}$ is defined as $L := A - D$. An undirected path is a sequence of ordered edges of the form $(v_{i_1}, v_{i_2}), (v_{i_2}, v_{i_3}), \ldots$, with $v_{i_j} \in \mathcal{V}$, $\forall j$. We denote with $\mathcal{V}_i \subset \{1, \ldots, N\}\backslash\{i\}$ the set of nodes connected with node i, for $i = 1, \ldots, N$. A graph $\mathcal{G}$ is called connected if and only if any two distinct nodes of $\mathcal{G}$ can be connected via a path, fully connected if and only if there is an edge connecting any two distinct nodes.

2. SYSTEM DESCRIPTION

Consider a broadcasting system, see [7], in which N encoded video streams are provided by N remote servers that share a communication channel of total transmission rate R_c, see Figure 1. The Media Aware Network Element (MANE) contains N dedicated buffers that temporarily store the encoded video streams, as Group of Pictures (GoP). The MANE contains the encoding rate controllers, and the transmission rate controllers. The encoding rate controllers limit the deviations of the current buffer level B_i from some reference level B_c, equal for all the streams. The transmission rate controllers adjust the drain rates of the

DOI: 10.1002/rnc

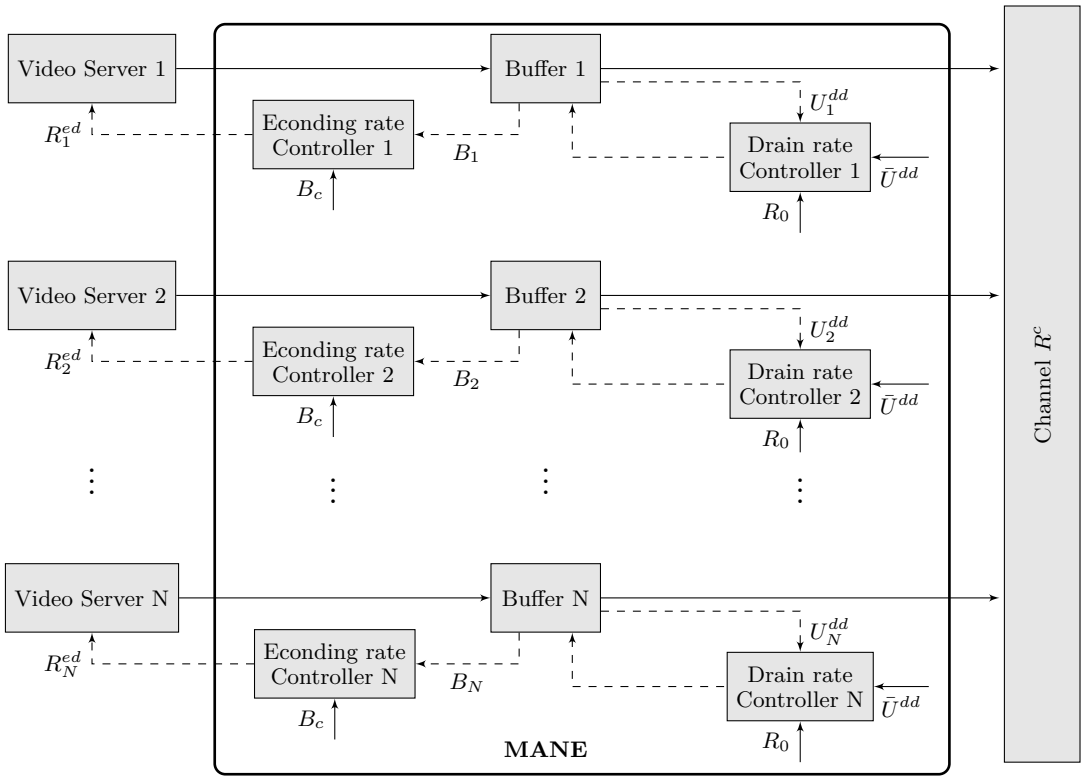

Figure 1. Structure of the quality-fair delivery system. The bold line delimits the MANE, that contains the buffers, the enconding rate, and transmission rate control loops.

buffers, using the the quality information of the stored GoP. There are several metrics to describe the video quality, like Peak Signal-to-Noise Ratio (PSNR) and Structural SIMilarity (SSIM) [36]. In video-on-demand services, these quality metrics can easily provided by the servers alongside the GoP. We call this quality information *utility*, denoted by U_i^{dd}, $i = 1, \ldots, N$. In the following, we assume that time is slotted with a period T and each video server is controlled synchronously, with GoPs of the same duration T. All propagations and queues in the system are modeled as time delays of duration T. Packet losses on the wireless post are assumed perfectly handled at the MAC layer.

The above setting leads to a discrete-time state-space representation of the controlled system, described by the following set of equations (conveniently reported from [7, equation (22)])

$$a_i(j)^+ = a_i(j) + \delta a_i(j) \tag{1a}$$
$$U_i^{dd}(j) = f(a_i(j), R_i^{edd}(j)) \tag{1b}$$
$$\Pi_i^b(j)^+ = \Pi_i^b(j) + (B_i(j) - B_c) \tag{1c}$$
$$R_i^{ed}(j)^+ = R_0 - \tfrac{K_P^{eb}+K_I^{eb}}{T}(B_i(j) - B_c) - \tfrac{K_I^{eb}}{T}\Pi_i^b(j) \tag{1d}$$
$$R_i^{edd}(j)^+ = R_i^{ed}(j) \tag{1e}$$
$$\Phi_i(j)^+ = \Phi_i(j) + \Delta U_i^{dd}(j) - U_i^{dd}(j) \tag{1f}$$
$$B_i(j)^+ = B_i(j) + [R_i^{edd}(j) - R_0 + (K_P^t + K_I^t)\Delta U^{dd}(j) - K_I^t \Phi_i(j)]T \tag{1g}$$
$$\Delta U_i^{dd}(j) = \bar{U}^{dd}(j) - U_i^{dd}(j) \tag{1h}$$
$$\bar{U}^{dd}(j) = \tfrac{1}{N}\textstyle\sum_{k=1}^{N} U_k^{dd}(j). \tag{1i}$$

DOI: 10.1002/rnc

Equations (1a)-(1b) constitutes the source model, that describes the nonlinear dependence of the utility output U_i^{dd} on the video-source characteristics a_i and on the encoding rate R_i^{edd} through the nonlinear function f. The quantity a_i models the time varying nature of the utility as a function of the encoding rate R_i^{edd}. The nonlinear function f is a continuous and increasing function of R_i^{edd}, which is the main nonlinearity of model (1). In this work we will design the PI gains by making a strong assumption on f, but we will illustrate our results on the full nonlinear time-varying model.

The encoding rate controller is characterized by (1c)-(1e), and it regulates the buffer level B_i around the reference level B_c. We assume that the reference encoding rate is $R_0 = \frac{R_c}{N}$, that is, the average rate, which would be allocated in a rate-fair scenario. The parameters K_P^e and K_I^e are the proportional and integral controller gains, respectively, corresponding to the first two parameters whose tuning is addressed in this paper.

Finally, the drain rate controller is described by (1g)-(1h). The buffer draining rate is updated comparing the utility function U_i^{dd} of the stream, with the mean value $\bar{U}^{dd}(j)$ in (1i) of the utilities of the overall system. The discrepancy between the utility function of the i-th video stream and the average utility of the network is described by (1h). The parameters K_P^t and K_I^t are the proportional and integral controller gains, respectively, corresponding to the second set of parameters tuned in this paper.

Problem statement. The goal of this work is to provide a systematic method to tune the PI controllers gains K_P^b, K_I^b, K_P^t, K_I^t in order to ensure the asymptotic convergence of the utilities $U_i(j)$ in (1b) to a common value $\bar{U}$, namely

$$\lim_{j\to+\infty} U_i^{dd}(j) = \bar{U}, \quad \forall i = 1, \dots, N. \tag{2}$$

The constant value $\bar{U}$ denotes the consensus value of the utilities. In comparison with the heuristic methods in the literature [7, 35], we want to give a systematic procedure for the design of the PI controllers gains, which also provides some desirable properties in terms of robustness with respect to the video characteristics variations of the delivered streams, and optimized for convergence to consensus.

Remark 1
We emphasize that the architecture of the MANE corresponds to a fully connected graph representation. Indeed, equation (1i) corresponds to a fully connected graph. Alternative distributed solutions may be indeed desirable and are certainly possible by using the tools proposed in this paper (they would simply refer to a different Laplacian matrix). In this work we stick with the current fully connected architecture because it corresponds to the technological structure of MANE, and because it allows for comparison with pre-existing works.

2.1. Two PI control loops

In this section we provide a state-space representation of model (1), in order to highlight the different actions performed by the encoding rate and transmission rate controllers on the network. We propose here a different change of coordinates of the system as compared to our preliminary work in [35], because this leads to a convenient formulation of the PI gains tuning in terms of an output feedback design problem, whose details are given in Section 4. Instead, in [35], the gain tuning procedure was merely heuristic.

The encoding rate controller (denoted by K_{int} in Figure 2, where "int" stands for "internal" loop) described by (1c)-(1e), is characterized by the following state space representation

$$\Pi_i^{b+} = \Pi_i^b + \Delta B_i \tag{3a}$$

$$\kappa_1 = \tfrac{k_I^{\text{int}}}{T}\Pi_i^b + \tfrac{k_P^{\text{int}}}{T}\Delta B_i, \tag{3b}$$

Prepared using rncauth.cls
DOI: 10.1002/rnc

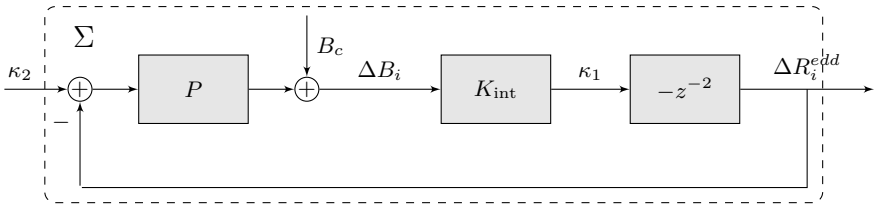

Figure 2. Block diagram representation of the encoding rate control loop for system (1). This loop is also called the "internal" loop, and denoted by Σ.

where Π_i^b is the controller state, $\Delta B_i = B_i - B_c$ is the controller input and $\kappa_1 = -\Delta R_i^{edd} = -(R_i^{edd} - R_0)$ is the controller output. The integral and proportional gains k_P^{int} and k_I^{int} are related to K_P^b, K_I^b according to the invertible relation

$$k_P^{\text{int}} = K_P^b + K_I^b, \quad k_I^{\text{int}} = K_I^b. \tag{4}$$

The encoding rate controller acts on the system (denoted by P in Figure 2) whose input-output relation is

$$\Delta R_i^{ed+} = \Delta R_i^e = -\kappa_1 \tag{5a}$$
$$\Delta R_i^{edd+} = \Delta R_i^{ed} \tag{5b}$$
$$\Delta B_i^{+} = \Delta B_i + T(\Delta R_i^{edd} - \kappa_2). \tag{5c}$$

In the sequel we denote with Σ the controlled system (3)-(5) from κ_2 to ΔR_i^{edd} (see Figure 2 and 3).

The transmission rate controller (denoted with K_{ext} in Figure 3, where "ext" stands for "external" loop), described by (1g)-(1i), provides the reference signal κ_2 to the closed-loop system (3)-(5) according to

$$\Phi_i^{s+} = \Phi_i^s + \tfrac{\Delta U_i^{dd}}{\rho} \tag{6a}$$
$$\kappa_2 = k_I^{\text{ext}}\Phi_i^s + \tfrac{k_P^{\text{ext}}}{\rho}\Delta U_i^{dd}, \tag{6b}$$

where $\rho > 0$ is a normalizing constant used for design purposes, $\Phi_i^s = \frac{\Phi_i}{\rho}$ is the controller state, $\Delta U_i^{dd} = U_i^{dd} - \bar{U}^{dd}$ is the controller input, and κ_2 is the controller output, and $\bar{U}^{dd}$ is defined in (1i) . The integral and proportional gains k_P^{ext} and k_I^{ext} are related to K_P^t, K_I^t according to the invertible relation

$$k_P^{\text{ext}} = \rho(K_P^t + K_I^t), \quad k_I^{\text{ext}} = \rho K_I^t. \tag{7}$$

Note that the integral actions of K_{int} and K_{ext} reject the constant reference buffer level B_c and the constant average encoding rate R_0, respectively.

From the structure of (3), (5), and (6), we notice that the overall system is composed by two nested control loops. The following state-space representation highlights the different

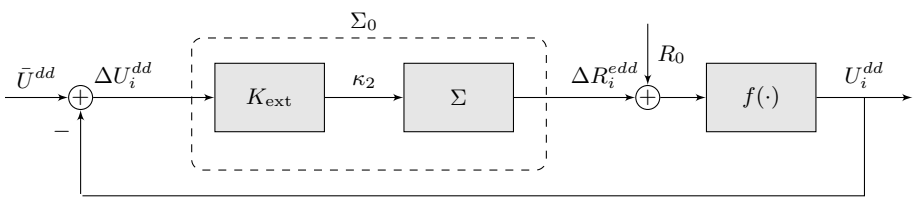

Figure 3. Block diagram representation of the draining rate control loop for system (1).

DOI: 10.1002/rnc

separate actions performed by controllers K_{int} and K_{ext}. Denote with $(A_{\text{int}}, B_{\text{int}}, C_{\text{int}}, D_{\text{int}})$ and $(A_{\text{ext}}, B_{\text{ext}}, C_{\text{ext}}, D_{\text{ext}})$ the matrices that characterize the state-space model of Σ and K_{ext}, respectively. Then, combining (3) and (5) for Σ and (6) for K_{ext}, we can represent the i-th video stream dynamics using the states

$$x_{\text{int},i} = \begin{bmatrix} \frac{\Delta B_i}{T} & \frac{\Pi_i}{T} & \Delta R_i^{ed} & -\Delta R_i^{edd} \end{bmatrix}^\top, \quad x_{\text{ext},i} = \Phi_i^s. \tag{8}$$

With this selection, the state-space matrices of Σ and K_{ext} are

$$\left(\begin{array}{c|c} A_{\text{int}} & B_{\text{int}} \\ \hline C_{\text{int}} & D_{\text{int}} \end{array}\right) = \left(\begin{array}{cccc|c} 1 & 0 & 0 & -1 & -1 \\ 1 & 1 & 0 & 0 & 0 \\ -k_P^{int} & -k_I^{int} & 0 & 0 & 0 \\ 0 & 0 & -1 & 0 & 0 \\ \hline 0 & 0 & 0 & -1 & 0 \end{array}\right), \tag{9}$$

$$\left(\begin{array}{c|c} A_{\text{ext}} & B_{\text{ext}} \\ \hline C_{\text{ext}} & D_{\text{ext}} \end{array}\right) = \left(\begin{array}{c|c} 1 & \frac{1}{\rho} \\ \hline k_I^{\text{ext}} & \frac{k_P^{\text{ext}}}{\rho} \end{array}\right). \tag{10}$$

Consider now the cascaded interconnection of K_{ext} and Σ (denoted with Σ_0 in Figure 3), which establishes the linear relation from ΔU_i^{dd} to ΔR_i^{edd}. A state-space representation of Σ_0 is given by

$$\left(\begin{array}{c|c} A_0 & B_0 \\ \hline C_0 & \end{array}\right) = \left(\begin{array}{cc|c} A_{\text{ext}} & 0 & B_{\text{ext}} \\ B_{\text{int}} C_{\text{ext}} & A_{\text{int}} & B_{\text{int}} D_{\text{ext}} \\ \hline 0 & C_{\text{int}} & \end{array}\right), \tag{11}$$

where matrix A_0 has a lower block-triangular structure. In particular, the eigenvalues of A_0 are the union of the eigenvalues of the diagonal blocks A_{int} and A_{ext}. This observation suggests that the two PI controllers act separately on the system dynamics: in particular controller K_{int} performs an internal stabilization of each video stream, while controller K_{ext} performs the external synchronization of the video streams utilities of the network.

3. NECESSARY AND SUFFICIENT CONDITIONS FOR CONSENSUS

In this section we cast the quality-fair delivery problem introduced in Section 2 into a consensus problem. More precisely, we want the network (1) to reach agreement on a quantity of interest, that is the utility function U_i of the video streams.

For instance, each system in (1) can be associated to a node in a graph $\mathcal{G} = (\mathcal{V}, \mathcal{E}, A)$, and it is an agent in the network. Each edge $(v_j, v_i) \in \mathcal{E}$ represents a communication link from agent i to agent j. The graph $\mathcal{G}$ is undirected (namely, the adjacency matrix satisfies $a_{ij} = a_{ji},\ \forall i \neq j$), as in the considered application each connection allows bidirectional communication between two agents.

The coupling among the agents arises from the average utility $\bar{U}_i^{dd}$ in (1i) of the video streams, acting as the reference input of the closed-loop system (see Figure 3). According to (1b), the quantity U_i^{dd} is a nonlinear function of the video-source parameters a_i and the encoding rate R_i^{edd}. It can be expressed as

$$U_i^{dd} = f(a_i, R_i^{edd}) = f(a_i, \Delta R_i^{edd} + R_0). \tag{12}$$

In this paper we make the following assumption, so that a linear time-invariant analysis of the consensus algorithm can be performed.

Assumption 1
For each $i = 1, \ldots, N$, a_i in (1a) is constant for each i. Moreover there exist scalars h_i, $i = 1, \ldots, N$ and a scalar $K_f > 0$ such that:

$$U_i^{dd} = f(a_i, R_i^{edd}) = h_i + K_f R_i^{edd} = h_i + K_f R_0 + K_f \Delta R_i^{edd}, \quad i = 1, \ldots, N. \tag{13}$$

DOI: 10.1002/rnc

Intuitively speaking, K_f translates the variation of utility provided by a variation of the video encoding rate, while the discrepancies between the rate-utility characteristics are captured by the coefficients h_i, for $i = 1, \ldots, N$.

Remark 2
The utility function depends on the particular video sequence, and different video coders may provide different utility characteristics of the same video sequence. Other multimedia traffic schemes model the utility function with different nonlinear approximations. As an example, [37, Section 2.3] considers a utility function that is logarithmic with the allocated rate. Using a different approach, [38] uses a non-differentiable utility function referred to as *staircase*. Alternatively, [39] adopts a sigmoidal-like utility function. In this paper, we adopt the affine approximation (13). This approximation is reasonable in some practical applications, like in MPEG-FGS video coders (see [40, Section 5.3.1]) for limited variations of the rate.

Based on Assumption 1 and on the integral action of controller K_{ext}, we may perform a coordinate change to compensate for the action of the constant disturbance $h_i + K_f R_0$, so that the overall system can be written as an output feedback network interconnection of N identical linear systems

$$\begin{array}{rcll} x_i^+ & = & A_0 x_i + B_0 \Delta U_i^{dd} & \\ U_i^{dd} & = & K_f C_0 x_i & i = 1, \ldots, N, \end{array} \tag{14}$$

where $x_i \in \Re^n$ is the state vector and U_i^{dd} the scalar output. Define the stacked column vectors

$$U^{dd} = \begin{bmatrix} U_1^{dd} & \ldots & U_N^{dd} \end{bmatrix}^\top, \; \Delta U^{dd} = \begin{bmatrix} \Delta U_1^{dd} & \ldots & \Delta U_N^{dd} \end{bmatrix}^\top. \tag{15}$$

The relation between ΔU^{dd} and U^{dd} in (15) can be rewritten in compact form using (1h) as

$$\Delta U^{dd} = -L U^{dd}, \tag{16}$$

where $L = [L_{ij}] \in \Re^{N \times N}$, and

$$L_{ij} = \begin{cases} \frac{N-1}{N}, & \text{if } i = j \\ -\frac{1}{N}, & \text{if } i \neq j. \end{cases} \tag{17}$$

The matrix L corresponds to the Laplacian matrix of the graph $\mathcal{G}$, which is *fully connected*, due to the centralized nature to the proposed control. This structure is intrinsic of the solution of the specific technological application and here reinterpreted in a consensus framework. Define the aggregate state vector $x = \begin{bmatrix} x_1^\top & \ldots & x_N^\top \end{bmatrix}^\top \in \Re^{Nn}$ and the aggregate output $y = \begin{bmatrix} y_1 & \ldots & y_N \end{bmatrix}^\top \in \Re^N$, where $y_i = U_i^{dd}$, for $i = 1, \ldots, N$. Combining (14) and (16), and using the Kronecker product, we obtain the following expression for the dynamics of the interconnected system

$$\begin{array}{rcl} x^+ & = & (I_N \otimes A_0) x - (L \otimes B_0) y \\ y & = & U^{dd} = (I_N \otimes K_f C_0) x, \end{array} \tag{18}$$

with A_0, B_0 and C_0 defined in (11). With the goal of establishing consensus, we define the consensus set

$$\mathcal{A} = \{ x \in \Re^{Nn} : x_i - x_j = 0, \quad \forall (i,j) \in \{1, \ldots, N\} \}. \tag{19}$$

and we recall that, given a set $\mathcal{A}$, we denote with $|\cdot|_{\mathcal{A}}$ the standard point-to-set distance $|x|_{\mathcal{A}} = \inf_{y \in \mathcal{A}} |x - y|$.

We are ready to give our main consensus result, in which we state a set of necessary and sufficient conditions for consensus for the identical discrete-time linear systems (14) with interconnection (16). As specified in (2), consensus in the above model means that all

DOI: 10.1002/rnc

the individual system utilities U_i^{dd} asymptotically reach a common value. This theorem is an extension of [35, Theorem 1]. This self-contained result provides a converse Lyapunov function theorem to prove consensus of the discrete-time linear closed-loop system (18). The main extension with respect to the preliminary work [35, Theorem 1] is the proof of the implication (i) $\implies$ (ii) of the following theorem, which is a converse Lyapunov result for the specific class of systems under consideration.

Theorem 1
Consider the closed-loop system (18). Under Assumption 1, the following statements are equivalent:

(i) Matrices A_{int} in (9) and
$$A_f = A_0 - \tfrac{N}{N-1} B_0 K_f C_0 \tag{20}$$
are Schur-Cohn.

(ii) There exists a quadratic Lyapunov function $V(x)$ for system (18) such that:
$$\begin{aligned} \bar{c}_1 \left|x\right|_{\mathcal{A}}^2 \leq V(x) \leq \bar{c}_2 \left|x\right|_{\mathcal{A}}^2 \\ \Delta V(x) \leq -\bar{c}_3 \left|x\right|_{\mathcal{A}}^2, \end{aligned} \tag{21}$$
for suitable positive constants $\bar{c}_1$, $\bar{c}_2$ and $\bar{c}_3$, and matrix A_{int} is Schur-Cohn.

(iii) The closed consensus set $\mathcal{A}$ in (19) is uniformly globally exponentially stable for the closed loop (18), and matrix A_{int} is Schur-Cohn.

(iv) The interconnected system (18) is such that the sub-states x_i uniformly globally exponentially synchronize to the unique solution to the following initial value problem
$$x_c^+ = A_0 x_c, \quad x_c(0) = \tfrac{1}{N} \textstyle\sum_{k=1}^N x_k(0), \tag{22}$$
and A_{int} is Schur-Cohn.

(v) Given any solution to (18), there exists $\bar{U} \in \mathbb{R}$ such that the output of (18) satisfies
$$\lim_{j \to +\infty} y_i(j) = \lim_{j \to +\infty} U_i^{dd}(j) = \bar{U}, \quad \forall i = 1, \ldots, N. \tag{23}$$

Proof
we first show a preliminary transformation, then we prove the theorem in five steps: (i) $\implies$ (ii), (ii) $\implies$ (iii), (iii) $\implies$ (iv), (iv) $\implies$ (v), and (v) $\implies$ (i).
Preliminary transformation. Let us introduce a suitable change of coordinates for the closed-loop system (18) (see, for example, [21]). Consider the symmetric matrix L in (16). There exists a unitary matrix $T \in \mathbb{R}^{N \times N}$ such that:
$$\Lambda = T^\top L T = \operatorname{diag}\left(\lambda_1, \ldots, \lambda_{N-1}, 0\right) = \operatorname{diag}\left(\lambda I_{N-1}, 0\right), \tag{24}$$
where we emphasized that L has $N-1$ eigenvalues equal to $\lambda = \frac{N}{N-1}$. Since the lower-right entry of Λ is zero, we select T such that its last column corresponds to the eigenvector $t_0 = \frac{1}{\sqrt{N}} \mathbf{1}_N$ associated to the zero eigenvalue of L. Furthermore, from the associative property of the Kronecker product, $T \otimes I_n$ transforms $L \otimes I_n$ into $\Lambda \otimes I_n$.

Consider system (18), and introduce the change of coordinates $\tilde{x} = (T^\top \otimes I_n) x$. Using the associative properties of the Kronecker product, dynamics (18) becomes
$$\begin{aligned} \tilde{x}^+ &= (T^\top T \otimes A_0)\tilde{x} - (T^\top L \otimes B_0) y && \text{(25a)} \\ y &= U^{dd} = (T \otimes K_f C_0)\tilde{x}. && \text{(25b)} \end{aligned}$$

DOI: 10.1002/rnc

Combining the equations in (25), and using (24) we obtain

$$\tilde{x}^+ = \left[(I_N \otimes A_0) - (\Lambda \otimes B_0 K_f C_0)\right] \tilde{x} = \begin{bmatrix} I_{N-1} \otimes \left(A_0 - \frac{N}{N-1} B_0 K_f C_0\right) & 0 \\ 0 & A_0 \end{bmatrix} \tilde{x}. \quad (26)$$

Proof of (i) $\implies$ (ii). By assumption, from the stability of A_f there exists a positive definite matrix $P_f \in \Re^{n \times n}$ such that:

$$A_f^\top P_f A_f - P_f = -I_n. \quad (27)$$

Consider the block diagonal matrix $P = \mathrm{diag}(I_{N-1} \otimes P_f, 0)$ and the Lyapunov function candidate:

$$V(x) = \underbrace{x^\top (T \otimes I_n)}_{\tilde{x}^\top} P \underbrace{(T^\top \otimes I_n)}_{\tilde{x}} = \sum_{k=1}^{N-1} \tilde{x}_k^\top P_f \tilde{x}_k. \quad (28)$$

From (27) and (28), the increment of $V(x)$ along the trajectories of (26) is

$$\Delta V(x) = \sum_{k=1}^{N-1} \tilde{x}_k^\top (A_f^\top P_f A_f - P_f) \tilde{x}_k = -\sum_{k=1}^{N-1} \tilde{x}_k^\top \tilde{x}_k. \quad (29)$$

To prove (21) we use [31][Lemma 1], after noticing that matrix T satisfies the assumption of this lemma. Then we also observe that, using matrix $\Delta = \mathrm{diag}(1, \ldots, 1, 0)$ defined in [31][Lemma 1], the last member in (29) writes

$$\sum_{k=1}^{N-1} \tilde{x}_k^\top \tilde{x}_k = \tilde{x}^\top (\Delta \otimes I_n) \tilde{x} = x^\top (T^\top \Delta T \otimes I_n) x. \quad (30)$$

Finally, from the positive definiteness of P_f, (30), and [31][Lemma 1], the Lyapunov function candidate (28) satisfies

$$c_2 \lambda_{\min} |x|_{\mathcal{A}} \leq \lambda_{\min} \sum_{k=1}^{N-1} |\tilde{x}_k|^2 \leq V(x) \leq \lambda_{\max} \sum_{k=1}^{N-1} |\tilde{x}_k|^2 \leq c_1 \lambda_{\max} |x|_{\mathcal{A}}, \quad (31)$$

for some positive constants c_1 and c_2, where $\lambda_{\min}$ and $\lambda_{\max}$ denote the minimum and maximum eigenvalue of P_f, respectively. Finally, using (29), (30) and [31][Lemma 1], we obtain

$$\Delta V(x) \leq -x^\top (T^\top \Delta T \otimes I_n) x \leq -c_1 |x|_{\mathcal{A}}^2. \quad (32)$$

We conclude that (21) is satisfied with $\bar{c}_1 = c_1 \lambda_{\min}$, $\bar{c}_2 = c_2 \lambda_{\max}$, and $\bar{c}_3 = c_1$.

Proof of (ii) $\implies$ (iii). Based on (28), the uniform global exponential stability of $\mathcal{A}$ in (19) follows from standard Lyapunov results (see, *e.g.*, the discrete- special cases of the hybrid results in [41, Theorem1]).

Proof of (iii) $\implies$ (iv). Consider the dynamics of the state $x_c(t) = \frac{1}{N} \sum_{k=1}^N x_k(t)$. Based on (14), the time evolution of x_c is

$$x_c^+(t) = \tfrac{1}{N} \textstyle\sum_{k=1}^N x_k^+(t) = A_0 \sum_{k=1}^N x_k(t) + B_0 \sum_{k=1}^N \Delta U_k^{dd}(t), \quad (33)$$

and from (16) we have that $\sum_{k=1}^N \Delta U_k^{dd} = \mathbf{1}_N^\top \Delta U^{dd} = -\mathbf{1}_N^\top L U_k^{dd} = 0$, since L has one zero eigenvalue relative to the left eigenvector $\mathbf{1}_N^\top$. From this observation, x_c evolves autonomously according to

$$x_c^+(t) = A_0 x_c(t), \quad (34)$$

that corresponds to the average of the states x_i in (14), with initial condition $x_c(0) = \frac{1}{N} \sum_{k=1}^N x_k(0)$. Since form (ii) $\implies$ (iii) the states x_i exponentially sunchronize to the same value, then for linearity they synchronize to their average value, i.e., (34).

Prepared using rncauth.cls
DOI: 10.1002/rnc

Proof of (iv) $\implies$ (v). Note that system (34) corresponds to Σ_0, whose state-space representation is given in (11). The state matrix A_0 has a block diagonal structure, therefore its eigenvalues are $\lambda(A_0) = \lambda(A_{\text{ext}}) \cup \lambda(A_{\text{int}}) = \{1\} \cup \lambda(A_{\text{int}})$. Since A_{int} is Schur-Cohn, all the solutions to (14), (16) converge to a constant.

Proof of (v) $\implies$ (i). We prove this statement by contradiction. Assume that (i) does not hold. We must analyze these two situations

- A_f is not Schur-Cohn. In this case consider the interconnected dynamics (26) in the transformed coordinates. Pick a vector $w^\star \in \Re^n$ (an eigenvector of the non-converging natural modes of A_f) such that the solution to (26) from $\tilde{x}^\star(0) := \begin{bmatrix} w^{\star\top} & 0 & \dots & 0 \end{bmatrix}^\top$ corresponds to $\tilde{x}^\star(t) := \begin{bmatrix} \tilde{x}_1^\top(t) & 0 & \dots & 0 \end{bmatrix}^\top$, for the block diagonal structure of the state matrix in (26). The function in (28) along this solution corresponds to

$$V(x^*(t)) = V((T \otimes I_n)\tilde{x}^*(t)) = \tilde{x}_1^\top(t) P_f \bar{x}_1(t),$$

  which, from linearity, remains bounded away from zero. Then, using the first inequality in (21) we have that $|x^*(t)|_{\mathcal{A}}$ is bounded away from zero, namely the solution $x^*(t)$ does not converge to the consensus set $\mathcal{A}$ in (19). This implies, according to (18), that the components of $y^\star(t) = (I_N \otimes K_f C_0) x^\star(t)$ do not synchronize, which contradicts (v).

- A_f is Schur-Cohn and A_{int} is not Schur-Cohn. We can trace the proofs (i) $\implies$ (ii) $\implies$ (iii) $\implies$ (iv) and say that all the solutions to (14), (16) synchronize to the solution to (34). Two cases may occur: **a)** A_{int} has at least one eigenvalue with magnitude larger than 1 or at least one eigenvalue on the unit circle with multiplicity larger than 1: in this case some solutions synchronize to a diverging evolution, thus item (v) does not hold; **b)** A_{int} has at least one eigenvalue with magnitude 1 on the unit disk. If that eigenvalue is at 1, then due to the triangular structure, matrix A_0 has two eigenvalues in 1 (the other one coming from A_{ext}) and again some solutions synchronize to a diverging evolution. If that eigenvalue is anywhere else in the unit circle, then it generates a revolving non-constant mode and some solutions synchronize to a non-convergent oscillatory trajectory. In both cases **a)** and **b)**, item (v) does not hold and the proof is completed.

□

Remark 3
Note that a discrete-time dead-beat controller using the knowledge of $\bar{U}^{dd}$ could achieve (2) in finite time, based on the knowledge of R_0, B_c and h_i. However, the filtering action of the double PI loop proposed in [7, 8] is more effective in dealing with the actual time-varying nature of (13), that can be well represented by suitable additional disturbances affecting the average behavior characterized by (13). That points out the relevance of the PI scheme.

Remark 4
The equivalent conditions contained in Theorem 1 establish the link between consensus in the original system (1) (under Assumption 1), and the closed-loop system (26) in the transformed coordinates. In fact, conditions (i)–(iv) are written based on the transformed coordinates (25), while the last condition (v) is based on the original system (1).

4. CONTROL DESIGN

In this section, we address the problem of finding a design procedure to select the value of the PI controller gains K_P^b, K_I^b, K_P^t, K_I^t, in order to guarantee the convergence of the

DOI: 10.1002/rnc

utilities U_i^{dd} to a common value—that is, (2). From Theorem (1), the design of the PI gains that guarantees (2) for the original system (1) under Assumption 1—that is, item (v) of Theorem 1—is equivalent to the simultaneous stabilization of the matrices A_{int} and A_f in (9) and (20), respectively—that is, item (i) of Theorem 1. Moreover, we would like to go one step further asking whether it is possible to optimize the PI controllers for faster convergence to consensus, which amounts to minimize the *spectral radius*—that is, the supremum among the absolute values of the eigenvalues— of A_f and A_{int}. This problem is known in the literature as the *generalized eigenvalue problem* (see [42]). More precisely, the problem of designing the PI controllers K_{int} and K_{ext} is translated here in terms of an optimized static output feedback design problem, through the equivalent characterization for consensus given in Theorem 1. In this section, we provide a systematic procedure to find the solution to the optimized static output feedback design problem. This procedure is described in Algorithm 1, which consists in iteratively solving a sequence of quasi-convex optimization problems. The proposed solution is of general applicability (see Remark 5) beyond the considered fair-delivery problem, and it can be viewed as an alternative approach to coordinate descent algorithms [43, 44]. The static output feedback problem is known in literature to be a challenging one, and, in general, there is no guarantee of existence of a stabilizing controller (see [45]). The existence of a feasible solution depends on the system data, and the particular architecture of the system under consideration. Although the solution of the static output feedback problem is not guaranteed to exist in general, the relevance of the PI scheme as technological solution to this specific problem suggests that the solution exists in practice. This observation is supported by the simulations shown in Section 5. The gain selection consists in a two-steps optimization process in which first the controller K_{int} is designed in order to maximize the convergence rate of A_{int}, and once K_{int} is fixed, the same procedure is applied to the selection of K_{ext}, in order to maximize the convergence rate of A_f. Note that, choosing the parameter $\rho = K_f \frac{N}{N-1}$, A_f becomes independent of the network parameters. After a suitable permutation of the state variables, matrices A_{int} in (9) and A_f in (20) can be conveniently rewritten as a function of the controllers $K_{\text{int}} = \begin{bmatrix} k_P^{\text{int}} & k_I^{\text{int}} \end{bmatrix}$ and $K_{\text{ext}} = \begin{bmatrix} k_I^{\text{ext}} & k_P^{\text{ext}} \end{bmatrix}$ as follows

$$A_{int} = A_1 - B_1 K_{\text{int}} C_1 \tag{35}$$

$$A_f = A_2 - B_2 K_{\text{ext}} C_2 \tag{36}$$

where we have defined

$$\left(\begin{array}{c|c} A_1 & B_1 \\ \hline C_1 & \end{array}\right) = \left(\begin{array}{cccc|c} 1 & 0 & 0 & -1 & 0 \\ 1 & 1 & 0 & 0 & 0 \\ 0 & 0 & 0 & 0 & 1 \\ 0 & 0 & -1 & 0 & 0 \\ \hline 1 & 0 & 0 & 0 & \\ 0 & 1 & 0 & 0 & \end{array}\right), \tag{37}$$

$$\left(\begin{array}{c|c} A_2 & B_2 \\ \hline C_2 & \end{array}\right) = \left(\begin{array}{ccccc|c} 1 & 1 & 0 & 0 & 0 & 0 \\ 0 & -1 & 0 & 0 & 1 & 1 \\ 0 & 0 & 1 & 0 & 1 & 0 \\ 0 & 0 & -k_I^{int} & 0 & -k_P^{int} & 0 \\ 0 & 0 & 0 & -1 & 0 & 0 \\ \hline 1 & 0 & 0 & 0 & 0 & \\ 0 & 1 & 0 & 0 & 0 & \end{array}\right). \tag{38}$$

A possible way to select the gains K_{int} and K_{ext}, exploiting the particular structure of matrices in (37) and (38), is given in Algorithm 1. The core idea is to alternate between two main steps, each of them requiring the solution to a quasi-convex optimization problem, i.e., a generalized eigenvalue problem (GEVP) based on LMI and bisection, where the controller gain K and a multiplier G are alternated as optimization variables. Algorithm 1 joins several useful properties that make it a promising tool for computing suboptimal selections of the static output feedback gains. Clearly, there is no guarantee of optimality, as the static output feedback problem is well known to be a challenging and nonconvex one. Some useful properties of Algorithm 1 are stated and proven next.

DOI: 10.1002/rnc

Algorithm 1 Convergence rate α and controller K

Input: Matrices A, B, $C = \begin{bmatrix} I & 0 \end{bmatrix}$, and a tolerance $\delta > 0$.
Initialization: Set $M = 0$ and initialize the pair $(\alpha_L, \alpha_H) = (\sigma_0, 1.1)$, where, using $\bar{\sigma}(A)$ to denote the maximum singular value of A, we select

$$\sigma_0 = 1 - \bar{\sigma}^2(A). \tag{39}$$

Pair (α_L, α_H) is *admissible* for (40), in the sense that (40) is feasible with $\alpha = \alpha_L$ and infeasible with $\alpha = \alpha_H$.
Iteration
Step 1: Given M and pair (α_L, α_H) from the previous step, solve, using bisection with tolerance $\delta > 0$, the GEVP

$$\begin{aligned} \max_{W, G_{11}, G_{21}, G_{22}, X_1, \alpha} \quad & \alpha \\ \text{s.t.} \quad & \begin{bmatrix} -W + \alpha W & AG - BX \\ \star & -G - G^\top + W \end{bmatrix} \leq 0, \end{aligned} \tag{40}$$

where $W = W^\top > 0$ and matrices, G and X have the following structure (see, for example, [44] for details on the use of multipliers)

$$G = \begin{bmatrix} G_{11} & G_{11}M \\ G_{21} & G_{22} \end{bmatrix}, X = X_1 \begin{bmatrix} I & M \end{bmatrix}. \tag{41}$$

In particular, determine an admissible pair (α_L, α_H) such that $\alpha_H - \alpha_L \leq \delta$. Pick the (sub)optimal solution $\bar{G}_{11}$, $\bar{X}_1$ corresponding to α_L, and set $\bar{K} = \bar{G}_{11}^{-1}\bar{X}_1$ for the next step.
Step 2: Given $\bar{K}$ and pair (α_L, α_H) from the previous step, set $\bar{A} = A - B\bar{K}C$, and solve, using bisection with tolerance $\delta > 0$, the GEVP

$$\begin{aligned} \max_{\alpha, W = W^\top > 0} \quad & \alpha \\ \text{s.t.} \quad & \bar{A} W \bar{A}^\top - W \leq -\alpha W. \end{aligned} \tag{42}$$

In particular, determine an admissible pair (α_L, α_H) such that $\alpha_H - \alpha_L \leq \delta$. Pick the (sub)optimal solution $\bar{W} = \begin{bmatrix} \bar{W}_{11} & \bar{W}_{12} \\ \bar{W}_{21} & \bar{W}_{22} \end{bmatrix}$ (where W has the partition induced by G), corresponding to α_L and set $M = \bar{W}_{11}^{-1}\bar{W}_{12}$ for the next step.
until α_L does not increase more than δ over three consecutive steps.
Output: $K_{out} = \bar{K}$ and $\alpha_{out} = \alpha_L$.

Proposition 1
The following statements hold:

(i) *Initialization and termination*: Given any input $\left(A, B, \begin{bmatrix} I & 0 \end{bmatrix}\right)$ and tolerance $\delta > 0$, the pair of scalars (α_L, α_H) defined in the Initialization step of Algorithm 1 is an admissible pair. Moreover, the algorithm terminates after a finite number of steps.

(ii) *Feasibility*: Given any admissible pair $(\alpha_{L_1}, \alpha_{H_1})$ from Step 1, the pair $(\alpha_{L_2}, \alpha_{H_2})$ obtained from the subsequent Step 2 always satisfies $\alpha_{L_2} \geq \alpha_{L_1}$, and vice versa.

(iii) *Guarantees*: Any solution (K_{out}, α_{out}) resulting from Algorithm 1 satisfies $\sigma\left(A - BK_{out}\begin{bmatrix} I & 0 \end{bmatrix}\right) \subseteq \mathbb{C}_{\leq \beta}$, where $\beta = \sqrt{1 - \alpha_{out}}$. In particular, if $\alpha_{out} > 0$, then

Prepared using rncauth.cls
DOI: 10.1002/rnc

the gain selection K_{out} is a stabilizing output feedback gain for the triple $(A, B, \begin{bmatrix} I & 0 \end{bmatrix})$, and β is the corresponding convergence rate.

Proof

Proof of (i). First, we prove that $(\sigma_0, 1.1)$ is an admissible pair in the sense clarified in the Initialization step. Trivially, (40) is infeasible with $\alpha > 1$, because the upper-left entry is positive. To show that (40) is feasible with $\alpha = \alpha_L = \sigma_0$ as in (39), select $G_{11} = I$, $G_{22} = I$, $G_{21} = 0$, $X_1 = 0$, and $W = I$ so that, applying a Schur complement, (40) is feasible if

$$(\sigma_0 - 1)\, I + AA^\top \leq 0, \tag{43}$$

which is clearly ensured if $\sigma_0 - 1 + \bar{\sigma}^2(A) \leq 0$. We now prove that the algorithm always terminates in a finite number of steps. Let $\alpha_{L_1}^j$ denote the value of α_L at the j-th iteration of Step 1. From item (ii) of Proposition 1 the sequence $\alpha_{L_1}^j$, $j \in \mathbb{N}$, is non decreasing and upper bounded by $\alpha = 1$, thus it is convergent. That is, given $\delta > 0$ there exists an index $j \in \mathbb{N}$ such that $\alpha_{L_1}^{j+1} - \alpha_{L_1}^j \leq \delta$.

Proof of (ii). [From Step 1 to Step 2]. By substituting the solution α_{L_1}, $\bar{K}$ obtained from Step 1 in (40) we get that

$$\begin{bmatrix} -W + \alpha_{L_1} W & (A - B\bar{K}C)G \\ \star & -G - G^\top + W \end{bmatrix} \leq 0 \tag{44}$$

has a feasible solution. By applying Finsler's Lemma, feasibility of (44) is equivalent to feasibility of

$$(A - B\bar{K}C)W(A - B\bar{K}C)^\top - W \leq -\alpha_{L_1} W. \tag{45}$$

Comparing (45) with (42), it follows that the subsequent solution α_{L_2} to Step 2 satisfies $\alpha_{L_2} \geq \alpha_{L_1}$.

[From Step 2 to Step 1]. Substitute the solution α_{L_2}, M obtained from Step 2 in (42) and perform a Schur complement to get

$$\begin{bmatrix} -W + \alpha_{L_2} W & (A - BKC)W \\ \star & -W - W^\top + W \end{bmatrix} \leq 0, \tag{46}$$

which corresponds to (40) with $W = G$. It follows that the subsequent solution α_{L_1} to Step 1 satisfies $\alpha_{L_1} \geq \alpha_{L_2}$.

Proof of (iii). From linear systems theory [46], we get that both solutions at Step 1 and Step 2 provide a certificate that matrix $\bar{A} = A - BK_{out}C$ has a spectral radius smaller than α_{out}. □

Remark 5

There is no loss of generality in considering systems in the form $(A, B, \begin{bmatrix} I & 0 \end{bmatrix})$ in Algorithm 1. For a system in a general form (A, B, C), where matrix C is full-row rank, there always exists a nonsingular matrix T such that $CT^{-1} = \begin{bmatrix} I & 0 \end{bmatrix}$. Using T as a similarity transformation we obtain $(T^{-1}AT, T^{-1}B, CT) = (\bar{A}, \bar{B}, \begin{bmatrix} I & 0 \end{bmatrix})$. Thus Algorithm 1 can be applied to any static output feedback design problem, underlining the general applicability of Theorem 1.

To demonstrate the effectiveness and the convergence of the proposed algorithm, the outer and inner loop gains K_{int} and K_{ext} of the quality-fair delivery application discussed on Section 2 are designed using the general procedure in Algorithm 1, with tolerance $\delta = 10^{-8}$, and with the selections in (37) and (38), respectively. Figure 4(top) shows that after 32 iterations, the rate α_L related to the selection of K_{int} (see (35), (37)) corresponds to 0.37789, with $K_{\text{int}} = \begin{bmatrix} 0.19256 & 0.012915 \end{bmatrix}$. Figure 4(bottom) shows similar results for the selection of K_{ext}: after 33 iterations the value of α_L is 0.1165 with $K_{\text{ext}} = \begin{bmatrix} 0.17645 & 0.65801 \end{bmatrix}$.

In our preliminary work [35] we used a graphical method to solve the design problem for K_{int} and K_{ext} with the same performance goal as that one of Algorithm 1. This algorithm provides similar results to those of [35] by using a systematic approach, which can be generalized to systems of any order, contrarily to the graphical method in [35].

Prepared using rncauth.cls
DOI: 10.1002/rnc

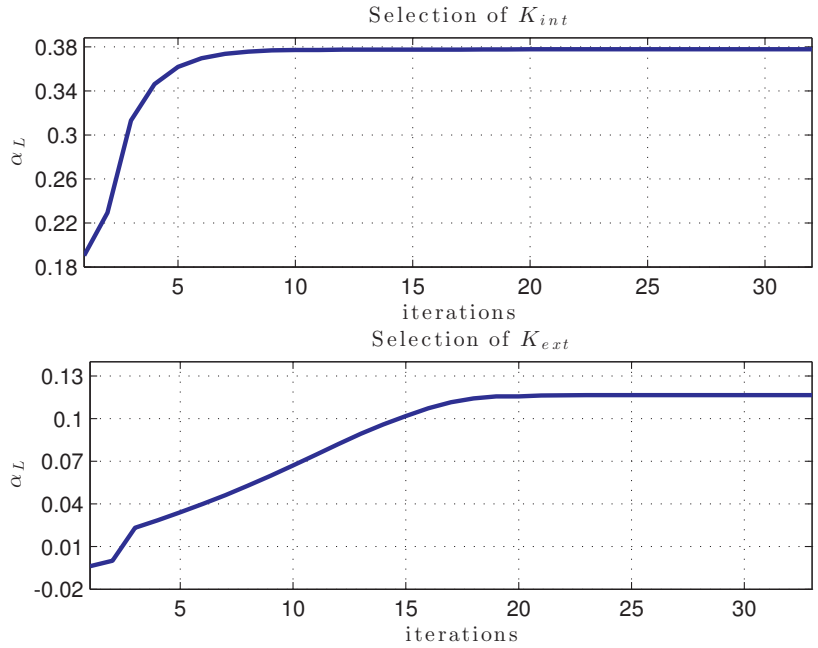

Figure 4. Gain selection via Algorithm 1. Evolution of the convergence rate α_L of A_{int} (top) and A_f (bottom).

5. SIMULATIONS

In this section we provide simulation results to demonstrate the effectiveness of the control design technique described in the previous section.

In the simulations we consider six video streams[†] of different types, encoded during 60 s with x.264 [47] in 4CIF (704×576) format at various bit rates. The programs are Interview (Prog 1), Sport (Prog 2), Big Buck Bunny (Prog 3), Nature Documentary (Prog 4), Video Clip (Prog 5), and an extract of Spiderman (Prog 6). The frame rate is $F = 30$ frames/s. We consider GoPs of 10 frames with duration $T = 0.33$ s, for a total number of GoP of $M = 180$. The model parameters are selected as follows: the reference buffer level is $B_c = 1200$ kb to tolerate significant variations of the buffering delay, and the channel rate is $R_c = 4000$ kb/s. The considered utility function U_i is the PSNR, and we evaluate the performance of the control schemes with the metric

$$\overline{\Delta U} = \frac{1}{MN} \sum_{j=1}^{M} \sum_{k=1}^{N} \left| U_k^{dd}(j) - \overline{U}^{dd}(j) \right|, \tag{47}$$

that is the time and ensemble average of the absolute value of the difference between the PSNR of each stream and the average PSNR of all the streams. A smaller value of $\overline{\Delta U}$ indicates a better performance of the control scheme, as it indicates that all the utilities are closer to the average for all the times.

We simulate the behavior of the servers, the network, the MANE, the BS, and the clients in Matlab. In the simulations we compare the following approaches:

PI1 *PI controllers with parameter tuning based on Theorem 1 and Algorithm 1.* We set the value of the parameter K_f in (13) as follows. We evaluate the time and ensemble average of the rate-PSNR characteristics for the four first streams at different constant encoding rates $R_i^{ed} = R^{ed}$, $i = 1, \ldots, 4$, in the range from 250 kb/s to 2 Mb/s. The

[†] http://www.youtube.com/watch?v=l2Y5nIbvHLs, =G63TOHluqno, =YE7VzlLtp-4, =NNGDj9IeAuI, =rYEDA3JcQqw, =SYFFVxcRDbQ.

DOI: 10.1002/rnc

resulting values of K_f are in the range from 0.02 dB/kb/s to 0.0025 dB/kb/s. Among these values, we select $K_f = 0.02$ dB/kb/s to avoid aggressive variations of the video encoding rate and increase robustness of the system.

PI2 *PI controllers with parameter tuning based on [8].* This tuning gives stable A_{int} but unstable A_f. Then Theorem 1 anticipates lack of consensus[‡].

TRF *Transmission Rate Fair approach*, obtained removing the transmission rate controllers ((1g)-(1h)) from (1). The PI gains K_P^b, K_I^b are selected as in [8]. In this simplified architecture, the transmission rate is constant for all programs. Also in this case Theorem 1 anticipates lack of consensus and lack of convergence of the utilities, that is, (2) is not satisfied. In fact A_f in (20) has poles at the limit of stability (indeed the scheme corresponds to $L = \mathbf{0}_{N\times N}$, with only zero eigenvalues).

UMMF *Utility max-min fair approach [2].* The encoding rate for each GoP is selected to maximize the minimum utility under a total rate constraint.

CMUM *Constrained mean utility maximization approach [5].* The encoding rate for each GoP is selected to maximize the average utility under a total rate constraint and considering also maximum utility discrepancies between programs. Compared to [5], we do not take into account temporal smoothness constraints, because the other approaches do not model them.

The value of the average PSNR discrepancies $\overline{\Delta U}$ for the simulations is given in Table I.

Figure 5 shows the time evolution of the utilities U_i of the first group of videos (Programs 1-4). Figure 6 shows the time evolution of the utilities U_i, of the second group of videos (Programs 3-6), using the schemes PI2 (left) and TRF (right). We do not show the simulations using the other schemes because they give similar results as compared to the correspondent ones in Figure 5.

Note that both the control methods PI2 and TRF do not stabilize the consensus set. It is not surprising that the utilities obtained with these schemes diverge (see Figure 6(left)) and do not converge (see Figure 6(right)), when sending Programs 3-6. For this reason we can not evaluate the corresponding value of $\overline{\Delta U}$ for the scheme PI2 (see Table I).

From Figures 5 and Table I we deduce that the UMMF and CMUM schemes give the best results in terms of PSNR discrepancies $\overline{\Delta U}$. The price to pay is the computational complexity. In fact these approaches require the availability at the MANE of the RUCs of the future GoP of each video stream, and thereby the solution at each time step of a non-linear, non-differentiable constrained optimization problem. We observe in Figure 5(bottom-left), that the UMMF technique causes large variations of the PSNR at some time instants. They are due to scene changes, which this scheme do not model.

Summarizing, the control design technique proposed in this paper performs worse than the UMMF and the CMUM schemes, and better than the heuristics PI2 and TRF. However, it has a very small computational complexity. In fact, without needing the RUCs information, it provides a reasonable fairness among programs: in most of the cases we observe discrepancies among programs of less than 5 dB. In addition, the proposed control is robust with respect of the variations of the video characteristics as compared with the PI2 and the TRF scheme.

6. CONCLUDING REMARKS

Necessary and sufficient conditions for the quality-fair delivery of video contents have been given for the considered broadcasting system. A general LMI-based iterative procedure is

[‡] Note that the gains in [8] had been heuristically tuned without any formal guarantee of convergence.

Prepared using rncauth.cls
DOI: 10.1002/rnc

	PI1	PI2	TRF	UMMF	CMUM
Progs 1−4	2.28	2.37	4.12	0.88	1.53
Progs 3−6	3.22	–	3.66	1.45	1.19

Table I. Comparison of the average absolute value of the utility discrepancy $\overline{\Delta U}$ obtained with different control schemes (values in dB).

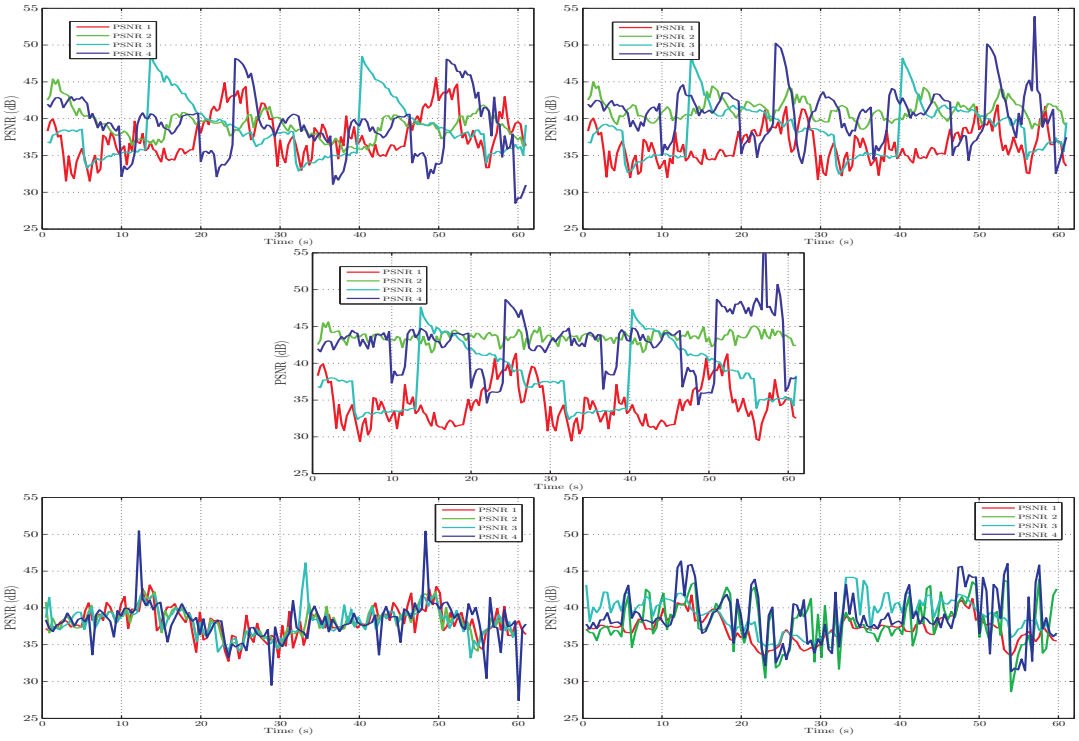

Figure 5. PSNR of Progs 1 to 4, comparison between different control schemes: PI1 (top left), PI2 (top right), TRF (middle), UMMF (bottom left), CMUM (bottom right).

.

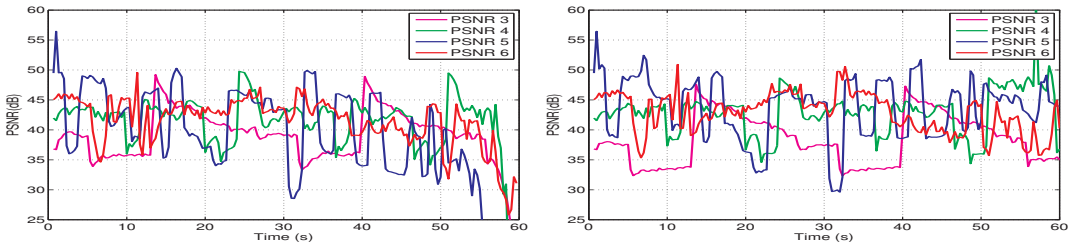

Figure 6. PSNR of Progs 3 to 6, comparison between the PI2 (left) and TRF (right).

addressed for the design of the two sets of PI gains of the technological solution proposed in the literature. This procedure has then been applied to determine the PI controller gains. Experimental results allow appreciating the advantages and the drawbacks of the proposed technique with respect to results of the literature. Future research directions will include relaxing Assumption 1, for example considering different approximating coefficients K_{f_i}, $i = 1, \ldots, N$, for each video stream, or taking into account the nonlinear nature of function f in (13).

DOI: 10.1002/rnc

REFERENCES

1. Index CVN. Forecast and methodology, 2009-2014. *Technical Report* 2010.
2. Cho J, Chong S. Utility max-min flow control using slope-restricted utility functions. *IEEE Global Comm. Conf.*, 2005; 818–824, doi:10.1109/GLOCOM.2005.1577753.
3. Li Y, Li Z, Chiang M, Calderbank A. Content-aware distortion-fair video streaming in congested networks. *IEEE Trans. Multimedia* October 2009; **11**(6):1182 –1193.
4. Cicalo S, Tralli V. Cross-layer algorithms for distortion-fair scalable video delivery over OFDMA wireless systems. *IEEE Global Comm. Conf.*, 2012; 1287–1292, doi:10.1109/GLOCOMW.2012.6477767.
5. Changuel N, Sayadi B, Kieffer M. Predictive encoder and buffer control for statistical multiplexing of multimedia contents. *IEEE Trans. Broadcast.* 2012; **58**(3):401–416.
6. Chen C, Zhu X, de Veciana G, Bovik AC, Heath RW. Rate adaptation and admission control for video transmission with subjective quality constraints. *IEEE J. Sel. Top. Signal Process.* feb 2015; **9**(1):22–36, doi:10.1109/jstsp.2014.2337277. URL http://dx.doi.org/10.1109/JSTSP.2014.2337277.
7. Changuel N, Sayadi B, Kieffer M. Control of distributed servers for quality-fair delivery of multiple video streams. *Proc. ACM Int. Conf. Multimedia*, Nara, Japan, 2012.
8. Changuel N, Sayadi B, Kieffer M. Control of multiple remote servers for quality-fair delivery of multimedia contents. *IEEE J. Select. Areas Commun.* Apr 2014; **32**(4):746–759, doi:10.1109/jsac.2014.140407.
9. Borcoci E, Negru D, Timmerer C. A novel architecture for multimedia distribution based on content-aware networking. *IEEE Int. Conf. on Comm. Theory Reliability Quality of Service*, 2010; 162 – 168, doi:10.1109/ctrq.2010.35.
10. Carli R, Chiuso A, Schenato L, Zampieri S. A PI consensus controller for networked clocks synchronization. *Proc. IFAC World Congr. 2008*, 2008; 10 289–10 294, doi:10.3182/20080706-5-kr-1001.01741.
11. Carli R, Zampieri S. Network clock synchronization based on the second-order linear consensus algorithm. *IEEE Trans. Autom. Control* February 2014; **59**(2):409–422.
12. Leonard N, Paley D, Lekien F, Sepulchre R, Fratantoni D, Davis R. Collective motion, sensor networks, and ocean sampling. *Proc. IEEE* 2007; **95**(1):48–74.
13. D'Innocenzo A, Di Benedetto MD, Serra E. Fault tolerant control of multi-hop control networks. *IEEE Trans. Autom. Control* 2013; **58**(6):1377–1389.
14. Moreau L. Stability of multiagent systems with time-dependent communication links. *IEEE Trans. Autom. Control* Feb 2005; **50**(2):169–182.
15. Jadbabaie A, Lin J, Morse A. Coordination of groups of mobile autonomous agents using nearest neighbor rules. *IEEE Trans. Autom. Control* June 2003; **48**(6):988–1001.
16. Olfati-Saber R, Murray R. Consensus problems in networks of agents with switching topology and time-delays. *IEEE Trans. Autom. Control* September 2004; **49**(9):1520–1533.
17. Ren W, Beard R. Consensus algorithms for double-integrator dynamics. *Distributed Consensus in Multi-vehicle Cooperative Control: Theory and Applications* 2008; :77–104.
18. Wieland P, Kim J, Scheu H, Allgöwer F. On consensus in multi-agent systems with linear high-order agents. *Proc. IFAC World Congr.*, vol. 17, 2008; 1541–1546.
19. Seo J, Shim H, JBack. Consensus of high-order linear systems using dynamic output feedback compensator: Low gain approach. *Automatica* nov 2009; **45**(11):2659–2664, doi:10.1016/j.automatica.2009.07.022.
20. Fax J, Murray R. Graph Laplacians and stabilization of vehicle formations. *Proc. of IFAC World Congr.* 2002; :88–88.
21. Fax J, Murray R. Information flow and cooperative control of vehicle formations. *IEEE Trans. Autom. Control* September 2004; **49**(9):1465–1476, doi:10.1109/TAC.2004.834433.
22. Wang J, Cheng D, Hu X. Consensus of multi-agent linear dynamic systems. *Asian J. Control* 2008; **10**(2):144–155.
23. Wang L, Xiao F. Finite-time consensus problems for networks of dynamic agents. *IEEE Trans. Autom. Control* April 2010; **55**(4):950–955.
24. Tuna S. LQR-based coupling gain for synchronization of linear systems. *arXiv preprint arXiv:0801.3390* 2008; .
25. Scardovi L, Sepulchre R. Synchronization in networks of identical linear systems. *Automatica* 2009; **45**(11):2557–2562.
26. Li Z, Duan Z, Huang L. Leader-follower consensus of multi-agent systems Jun 2009; :3256–3261.
27. Hong Y, Chen G, Bushnell L. Distributed observers design for leader-following control of multi-agent networks. *Automatica* 2008; **44**(3):846–850.
28. Zhang H, Lewis F, Das A. Optimal design for synchronization of cooperative systems: state feedback, observer and output feedback. *IEEE Trans. Autom. Control* 2011; **56**(8):1948–1952.
29. Liu Y, Jia Y, Du J, Yuan S. Dynamic output feedback control for consensus of multi-agent systems: An H_∞ approach. *Proc. American Control Conf.*, 2009; 4470–4475.
30. Li Z, Duan Z, Chen G, Huang L. Consensus of multiagent systems and synchronization of complex networks: a unified viewpoint. *IEEE Trans. Circuits Syst.* 2010; **57**(1):213–224.
31. Dal Col L, Tarbouriech S, Zaccarian L, Kieffer M. Equivalent conditions for synchronization of identical linear systems and application to quality-fair video delivery. *HAL-01116971 document* 2015; .
32. Xia T, Scardovi L. Synchronization conditions for diffusively coupled linear systems. *Int. Symposium on Mathematical Theory of Networks and Systems*, 2014; 1070–1075.
33. Wieland P, Sepulchre R, Allgöwer F. An internal model principle is necessary and sufficient for linear output synchronization. *Automatica* March 2011; **47**(5):1068–1074.

34. Blondel V, Tsitsiklis J. NP-hardness of some linear control design problems. *Proc. Conf. Decis. Control*, 1995, doi:10.1109/cdc.1995.478584.
35. Dal Col L, Tarbouriech S, Zaccarian L, Kieffer M. A linear consensus approach to quality-fair video delivery. *Proc. Conf. Decis. Control*, Los Angeles, 2014.
36. Wang Z, Bovik A, Sheikh H, Simoncelli E. Image quality assessment: from error visibility to structural similarity. *IEEE Trans. Image Process.* apr 2004; **13**(4):600–612, doi:10.1109/tip.2003.819861.
37. Lee KT, Tsai WH, Liao HYM, Chen T, Hsieh JW, Tseng CC. *Advances in Multimedia Modeling*. Springer, 2011.
38. Talebi MS, Khonsari A, Hajiesmaili MH, Jafarpour S. A suboptimal network utility maximization approach for scalable multimedia applications. *IEEE Global Telecom. Conf.*, 2009; 1–6.
39. Lee JW, Mazumdar RR, Shroff NB. Non-convex optimization and rate control for multi-class services in the internet. *IEEE Trans. Networking* 2005; **13**(4):827–840.
40. Ibnkahla M. *Adaptation and Cross Layer Design in Wireless Networks*. CRC press, 2008.
41. Teel A, Forni F, Zaccarian L. Lyapunov-based sufficient conditions for exponential stability in hybrid systems. *IEEE Trans. Autom. Control* 2013; **58**(6):1591–1596.
42. Boyd S, El Ghaoui L. Method of centers for minimizing generalized eigenvalues. *Linear Algebra Appl* 1993; **188**:63–111.
43. Arzelier D, Peaucelle D. An iterative method for mixed H_2/H_∞ synthesis via static output-feedback. *Proc. Conf. Decis. Control*, vol. 3, IEEE, 2002; 3464–3469.
44. Ebihara Y, Peaucelle D, Arzelier D. *S-variable approach to LMI-based robust control*. Springer, 2015.
45. Syrmos V, Abdallah C, Dorato P, Grigoriadis K. Static output feedback—a survey. *Automatica* feb 1997; **33**(2):125–137, doi:10.1016/s0005-1098(96)00141-0. URL http://dx.doi.org/10.1016/S0005-1098(96)00141-0.
46. Hespanha J. *Linear systems theory*. Princeton Press: Princeton, New Jersey, 2009.
47. x264 Home Page. Videolan organization 2011. http://www.videolan.org/developers/x264.html.